

Reduction of photoreceptor cell packing density in low or moderate myopia detected with adaptive optics scanning laser ophthalmoscopy

Lin-Yi Lei^{1,2}, Yue Zhao¹, Tang-Ren Cai^{1,2}, Si-Guo Feng^{1,2}, Jin Yao¹

¹The Affiliated Eye Hospital of Nanjing Medical University, Nanjing 210029, Jiangsu Province, China

²The Fourth School of Clinical Medicine, Nanjing Medical University, Nanjing 210029, Jiangsu Province, China

Co-first authors: Lin-Yi Lei and Yue Zhao

Correspondence to: Jin Yao. The Affiliated Eye Hospital of Nanjing Medical University, Nanjing 210029, Jiangsu Province, China. dryaojin@126.com

Received: 2024-04-20 Accepted: 2024-11-19

Abstract

• **AIM:** To assess the variations in photoreceptor cell packing density (PCPD) across the retina among young healthy individuals with emmetropia, low and moderate myopia.

• **METHODS:** High-resolution adaptive optics scanning laser ophthalmoscopy (AOSLO) systems were utilized for retinal imaging with a large sampling window of 700 $\mu\text{m} \times 700 \mu\text{m}$. The study cohort included 14 emmetropic [spherical equivalent (SE) ranged +0.5 to -0.5 D], 15 low myopic (SE ranged -0.5 to -3 D) and 21 moderate myopic (SE ranged -3 to -6 D) healthy young adults. Photoreceptors at 3° temporal, 6° superior and inferior 6° were captured. Statistical analysis was then performed to obtain PCPD and cell spacing.

• **RESULTS:** The average age of participants was 22.54 \pm 2.86 (ranged 20–30y) with no difference among 3 groups. At 3° temporal, the emmetropic group exhibited the highest PCPD of 15 186.16 \pm 2050.54 cells/mm², while the low and moderate myopic groups had PCPD of 14 009.15 \pm 1073.01 and 13 466.92 \pm 1121.71 cells/mm², respectively. At 3° temporal, the emmetropic group also had the smallest cell spacing at 6.66 \pm 0.26 mm, compared to 6.85 \pm 0.26 and 6.91 \pm 0.28 mm for the low and moderate myopic groups, respectively. Compared to the emmetropic group, at 3° temporal, the myopic groups showed significantly reduced PCPD (low myopia: $P=0.032$; moderate myopia: $P=0.001$). At 6° inferior, the moderate myopic group exhibited a significant decrease in PCPD ($P=0.013$), while at 6° superior, there were no significant

statistical differences in PCPD for the low and moderate myopic groups ($P>0.05$). In comparison to the emmetropic group, only the moderate myopic group showed significantly increased cell spacing at all three positions (temporal 3°: $P=0.011$, superior 6°: $P=0.046$, inferior 6°: $P=0.013$). Correlation analysis revealed a positive correlation between PCPD and axial length changes ($P<0.05$).

• **CONCLUSION:** Reduced PCPD and increased cell spacing strongly correlated with refractive error in mild to moderate myopic eyes, especially at 6° inferior to the fovea and the decreased PCPD in the macular region of myopic patients may be associated with increased axial length-induced retinal stretching.

• **KEYWORDS:** adaptive optics scanning laser ophthalmoscopy; photoreceptor cell packing density; fovea; refractive error; myopia

DOI:10.18240/ijo.2025.04.15

Citation: Lei LY, Zhao Y, Cai TR, Feng SG, Yao J. Reduction of photoreceptor cell packing density in low or moderate myopia detected with adaptive optics scanning laser ophthalmoscopy. *Int J Ophthalmol* 2025;18(4):683-690

INTRODUCTION

Myopia can be categorized into two distinct types, namely axial myopia and refractive myopia, with its onset typically manifesting during childhood^[1]. The global prevalence of myopia is on the rise, with significant rates observed in various regions of East Asia and Southeast Asia, where as many as 70% to 80% of young individuals demonstrate the condition of nearsightedness. Furthermore, around 20% of high school graduates are affected by severe myopia, which puts them at a higher risk for developing ocular conditions that can potentially lead to vision loss^[2-5]. Therefore, it is crucial to understand the anatomical changes associated with myopia in order to develop strategic plans aimed at reducing its prevalence. Addressing the increasing global incidence of myopia is recognized as an immediate concern that requires urgent attention^[1,6].

Since 2000, adaptive optics technology has been applied in clinical settings. Its integration with scanning laser ophthalmoscopy^[7] has furnished a crucial instrument for scrutinizing photoreceptor morphology in both healthy and diseased eyes, thereby advancing our comprehension of the mechanisms underlying photoreceptor degeneration and loss^[8]. This technology improves the quality and resolution of retinal imaging by real-time measurement and compensation of ocular aberrations, allowing researchers to observe and study microstructures within the visual system in real time, such as individual cells or cell layers within the retina^[8-10]. In contrast to in vitro histological analysis, adaptive optics scanning laser ophthalmoscopy (AOSLO) enables reproducible measurements that can be utilized for monitoring cellular-level retinal changes during myopia development^[11-13].

At present, optical correction can effectively restore clear vision in most cases of myopia. However, multiple studies have consistently demonstrated visual receptor dysfunction linked to myopia, including a reduction in photoreceptor sensitivity^[14-15]. Rossi *et al*^[16] discovered that despite the implementation of adaptive optics for correcting optical blur, myopia still exhibits a significantly compromised minimum resolution angle. This visual impairment can be attributed to the reduction in nerve sampling density associated with retinal stretching^[17]. Hence, it is crucial to obtain a more comprehensive understanding of how changes in eye length affect photoreceptor cell packing density (PCPD) within and surrounding the macular fovea.

Although data quantifying photoreceptor cells in the parafoveal area of the retina in myopic patients using AOSLO technology are available, establishing baseline values for large-scale imaging is challenging due to significant individual variations in PCPD at specific locations^[18]. Chui *et al*^[18] measured cone cell density within the range of 0.30–3.40 mm eccentricity from the fovea in myopic eyes (+0.50 to -7.50 D) but only included 11 patients. Woog and Legras^[19] observed changes in PCPD in 55 healthy individuals with varying eccentricities of refractive error, but they focused on the horizontal meridian at 24° eccentricity and did not include the vertical meridian range. Therefore, the aim of this study is to evaluate changes in PCPD and cell spacing in the temporal 3°, superior 6°, and inferior 6° regions in healthy adults with low to moderate myopia.

PARTICIPANTS AND METHODS

Ethical Approval The study adhered to the principles outlined in the Declaration of Helsinki and received approval from the Institutional Ethics Committee of Eye Hospital of Nanjing Medical University (No.2023001). Prior to the commencement of experimental measurements, the subjects were thoroughly briefed on all procedures and provided their written informed consent. Although the sample size was deemed sufficient for the AOSLO study, it may have been considered small when

generalizing the results to a broader population. Therefore, we acknowledged this as a limitation of the research.

Participants This study included 50 healthy subjects aged between 20 and 30y from China. All participants underwent a conventional eye examination, which comprised slit lamp examination, ophthalmoscopy, best-corrected visual acuity (BCVA), intraocular pressure (IOP) measurement, axial length (AL) assessment, refraction measurement and optical coherence tomography (OCT) examination. Refraction measurement was considered a subjective measure. The AL was measured using the intraocular lens (IOL) Master. All subjects exhibited BCVA of 20/20 or better. The IOP was all within the normal ranges for each group. The degree of astigmatism in the subjects was less than 1.00 D, which did not affect the imaging quality of AOSLO. Only one eye of each subject was included in the study. The exclusion criteria encompassed the presence of retinal pathology or systemic diseases, as well as the exclusion of individuals with suboptimal imaging quality. Additionally, subjects with atypical AL for their refractive status were excluded. The AL of the 50 subjects ranged from 22.78 to 25.89 mm [mean 24.51 mm; standard deviation (SD) 0.74]. Subjects were stratified into three cohorts based on their spherical equivalent (SE): 14 individuals classified as emmetropes (mean SE: -0.09, SD=0.16), 15 categorized as low myopias (mean SE: -1.61, SD=0.68), and 21 identified as moderate myopias (mean SE: -3.90, SD=0.82). All sample collections were performed under adequate paralysis of the ciliary muscle.

Apparatus Photoreceptor images were acquired using the AOSLO system (Mona IIa; Robotrak Technologies Co., Ltd., Device Software Version: V1.00.00.221118). In brief, the AOSLO imaging and wavefront sensor utilized a common 840 nm light source (840 nm SLD, FWHM-40 nm) with a field of view on the retina measuring 2.4°×2.4° (~700 μm×700 μm). The imaging system was designed to operate over a 7 mm exit pupil. The scanning process in this system involved an 8 kHz resonant scanner mirror for horizontal beam scanning and a 14 Hz galvo mirror for vertical scanning, resulting in a frame rate of 14 Hz. Prior to detection, a confocal pinhole with a diameter approximately equal to two Airy disks was positioned before an Avalanche Photodiode detector. To correct ocular aberrations, a high-speed deformable mirror was employed in conjunction with a customized Shack-Hartmann wavefront sensor. The imaging power entering the subject's pupil was maintained below 600 μW, which was well below the limits defined by American National Standards Institute (ANSI) standards.

Differences in AL and corrective lenses introduced variations in optical magnification, resulting in discrepancies between pixel coordinates and retinal dimensions (expressed in mm) measured by AOSLO. When comparing retinal dimensions for

a given visual angle, it was observed that the dimensions were larger in myopic retinas compared to emmetropic retinas due to the longer AL. This larger retinal dimension had implications for the calculation of PCPD in cells/mm². To address this, AOSLO employed a standard reduced eye model to calculate the retinal magnification factor. By utilizing calculations from Littmann's formula, the retinal magnification system was employed to rectify this discrepancy. To address this issue, AOSLO utilized the Littmann formula to calculate the retinal magnification factor, thereby correcting for these differences.

Procedures The imaging field captured was 2.4°×2.4°, corresponding to a size of 700 μm×700 μm. For each participant, we collected photoreceptor images at three locations: first, the area 3° temporal to the fovea where imaging was clearest, and then at 6° superior and inferior to the fovea. The region of interest was shown in Figure 1. Each set started at the fovea and proceeded towards the periphery along the meridian. Then AO detect was used to analyze PCPD and photoreceptor spacing. The same location was sampled on five occasions, and the corresponding measurements were recorded. All images achieved a real-time signal strength convergence of over 90%, ensuring the quality and reliability of the final images. Throughout the study, all examinations were conducted by a physician specialized in ocular functional imaging, who had completed training provided by Robotrak and had passed the qualification certification for clinical research using the device. The complete AOSLO imaging procedure for each participant lasted approximately 20 to 35min. The image data PCPD referred to the ratio of the number of photoreceptors in a given area to the size of that area. Cell spacing represented the average distance between each photoreceptor cell and its neighboring cells. In our study, we utilized a 2.4°×2.4° (700 μm×700 μm) window to capture the morphology and distribution of photoreceptors. Given the potential benefits of enhancing clinicians' ability to promptly identify pertinent areas and acquire comprehensive images of critical regions, the adoption of larger data windows may offer enhanced value in clinical practice.

Statistical Analysis All statistical analyses were performed using SPSS for Windows version 26. A *P* value <0.05 was considered statistically significant. The mean and standard deviation of continuous variables were determined. Results were expressed as mean±standard deviation. The Chi-square test, Student's *t*-test, and nonparametric Mann-Whitney-Wilcoxon test were used to compare the demographic and clinical data between the two groups. Using linear regression analysis, we investigated the correlation between PCPD, cell spacing, AL, and refractive error.

RESULTS

The study comprised 14 emmetropes, 15 low myopes, and

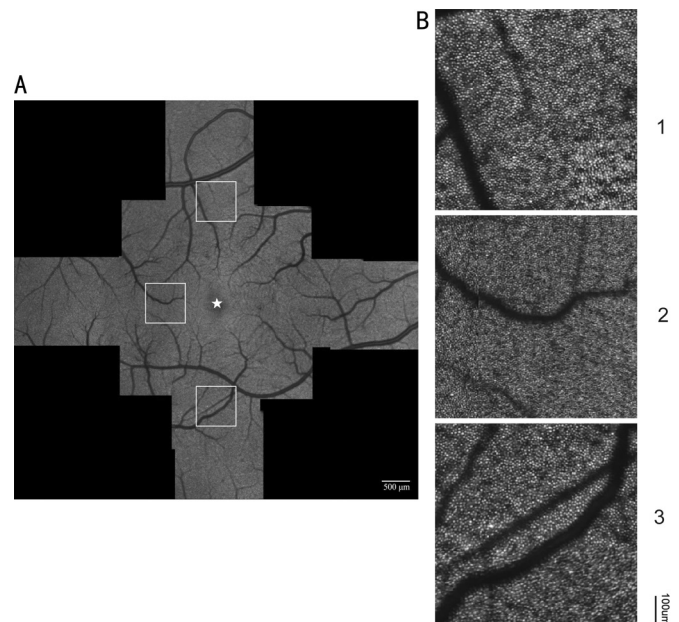


Figure 1 Illustrative examples of AOSLO images A: The montage captured from the foveal center (*) to the peripheral region. Numbers 1, 2, and 3 indicated eccentricities of superior 6°, temporal 3°, and inferior 6°. B: The high-resolution AOSLO image was acquired within the boxed region in A. The high-resolution AOSLO image revealed a clear resolution of photoreceptors at each retinal location, exhibiting a nearly continuous and regularly arranged photoreceptor mosaic pattern. AOSLO: Adaptive optics scanning laser ophthalmoscopy.

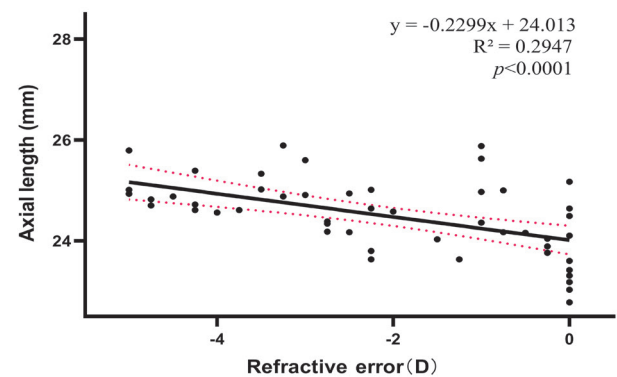


Figure 2 The correlation between axial length (mm) and spherical equivalent refractive error (D) in subjects' test eyes The solid line represents the linear regression of the data.

21 moderate myopes, all of whom were healthy Han Chinese young adults aged between 20 and 30y (22.54±2.86y) with a BCVA of 20/20 or better. There were no significant differences in terms of factors including gender, age, BCVA, and IOP. A significant negative correlation was observed between AL and refractive error ($R^2=0.2947$, $P<0.0001$). The correlation between refractive error and AL was illustrated in Figure 2. The main clinical characteristics of the three groups of subjects were shown in Table 1.

The retinal regions collected for analysis included the temporal area 3° from the fovea, as well as the superior and inferior regions 6° from the fovea. In emmetropic individuals,

Photoreceptor cell packing density with myopia

Table 1 Clinical characteristics of subjects

Group	<i>n</i>	Sex (M/F)	Age (y)	BCVA (logMAR)	IOP (mm Hg)	AL (mm)	SE (D)	mean±SD
Emmetrope	14	3/11	22.50±3.35	0.00±0.00	15.48±3.65	23.83±0.67	-0.09±0.16	
Low myopia	15	6/9	23.00±2.95	0.00±0.00	14.02±1.46	24.56±0.68	-1.61±0.68	
Moderate myopia	21	2/19	22.24±2.53	0.01±0.04	15.13±2.82	24.92±0.46	-3.90±0.82	
<i>F/χ²</i>		<i>χ²</i> =4.174	<i>F</i> =0.304	<i>F</i> =0.682	<i>F</i> =1.128	<i>F</i> =14.472	<i>F</i> =149.958	
<i>P</i>		0.151	0.739	0.511	0.332	<0.001	<0.001	

BCVA: Best-corrected visual acuity; IOP: Intraocular pressure; AL: Axial length; SE: Spherical equivalent.

Table 2 Mean PCPD and cell spacing in retinal areas across refractive error groups

Parameters	Group	Temporal 3°	Superior 6°	Inferior 6°	mean±SD
PCPD (cell/mm ²)	Emmetrope	15186.16±2050.54	9770.88±1240.18	9713.73±1280.92	
	Low myope	14009.15±1073.01	9715.84±2044.25	9225.53±1484.55	
	Moderate myope	13466.92±1121.71	8718.22±1509.39	8397.74±1423.65	
	Average	14110.98±1571.40	9337.00±1673.13	9025.92±1483.76	
Cell spacing (mm)	Emmetrope	6.66±0.26	7.19±0.48	7.11±0.49	
	Low myope	6.85±0.26	7.47±0.74	7.32±0.51	
	Moderate myope	6.91±0.28	7.64±0.59	7.53±0.44	
	Average	6.82±0.28	7.46±0.63	7.34±0.50	

PCPD: Photoreceptor cell packing density.

the highest PCPD in the retina is observed at temporal 3° with a measurement of 15 186.16±2050.54 cells/mm². Subsequently, the PCPD decreases to 9770.88±1240.18 and 9713.73±1280.92 cells/mm² at superior 6° and inferior 6° along the vertical meridian of the retina respectively. The corresponding cell spacing increased from 6.66±0.26 to 7.19±0.48, and 7.11±0.49 mm. In the temporal 3° region, PCPD is highest in emmetropic eyes at 15 186.16±2050.54 cells/mm². With increasing refractive error, PCPD decreases to 14 009.15±1073.01 and 13 466.92±1121.71 cells/mm², respectively. The cell spacing increases from 6.66±0.26 mm to 6.85±0.26 and 6.91±0.28 mm. Table 2 presented the mean photoreceptor densities, cell spacing among emmetropes, low myopias, and moderate myopes at three eccentricities. To highlight the changes in photoreceptors, AOSLO images were randomly selected from the eyes of participants in each refractive error group. The images collected by different ametropia groups at temporal 3°, superior 6°, and inferior 6° were depicted Figure 3. The density of photoreceptors decreases, while cell spacing increases, as eccentricity and refractive error progress.

The significant difference was evaluated using a one-way ANOVA analysis conducted in SPSS 26.0. It was performed to assess the significance of PCPD and cell spacing across the three groups. The distribution of PCPD and intercellular spacing among different visual acuity groups was presented in box plots. Figure 4 revealed that compared to emmetropes, there was a significant statistical difference in PCPD at temporal 3° in the mild myopia group, with a decreasing trend. In the moderate myopia group, there were significant

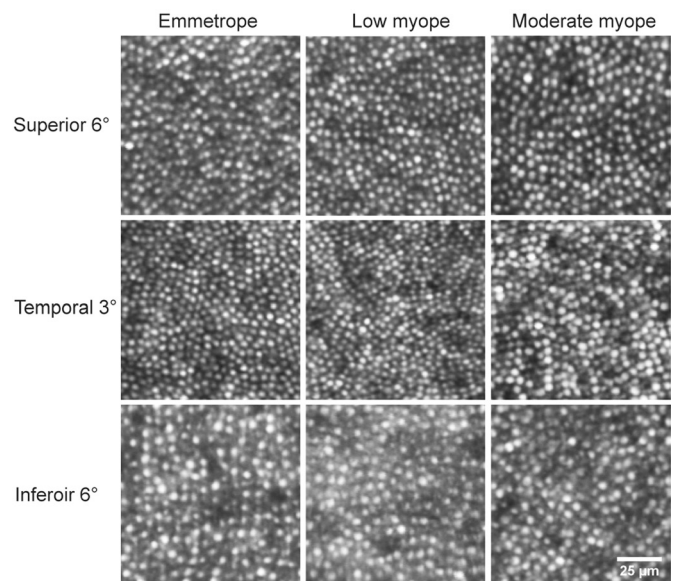


Figure 3 Representative images of PCPD variations across refractive error groups and eccentricities Analysis of typical images from three refractive error groups at temporal 3°, superior 6°, and inferior 6° relative to the fovea revealed a reduction in PCPD with increasing eccentricity, as well as variations in PCPD among the different refractive error groups. PCPD: Photoreceptor cell packing density.

statistical difference in PCPD at temporal 3° and inferior 6°, both showing a decreasing trend ($P<0.05$). When compared to emmetropes, the moderate myopia group displayed a significant increase in photoreceptor cell spacing in all three locations ($P<0.05$), whereas the mild myopia group did not exhibit a significant statistical increase.

PCPD (cell number/mm²) and cell spacing (mm) as a function of AL (mm) and refractive error (D) for three regions were

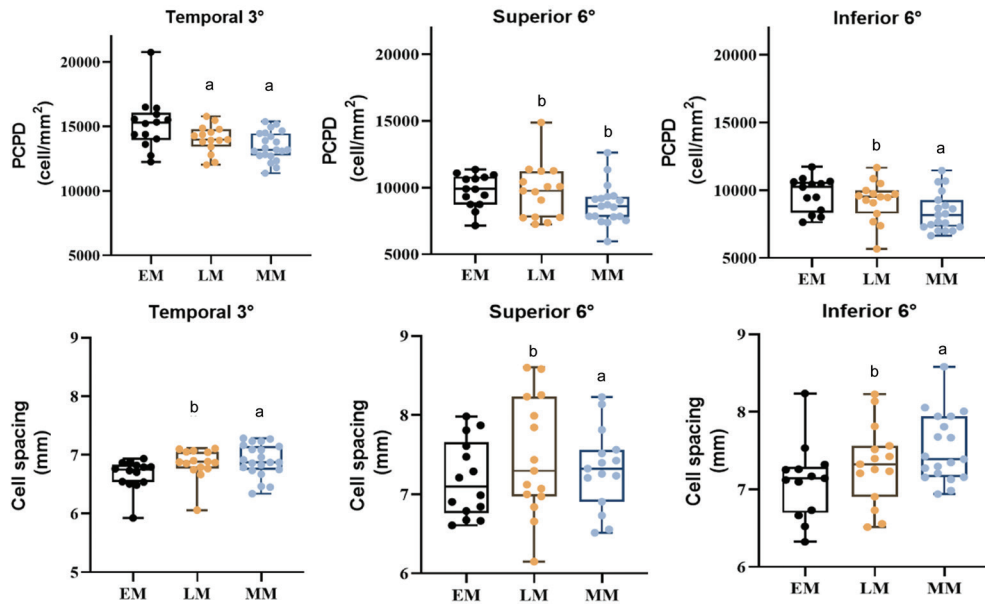


Figure 4 Distribution of PCPD and cell spacing across visual acuity groups: box plot analysis The median (black line) and interquartile range for each box were clearly visible. ^a $P < 0.05$ compared to the emmetropic group; ^bNo statistically significant difference. PCPD: Photoreceptor cell packing density; EM: Emmetropic; LM: Low myopic; MM: Moderate myopic.

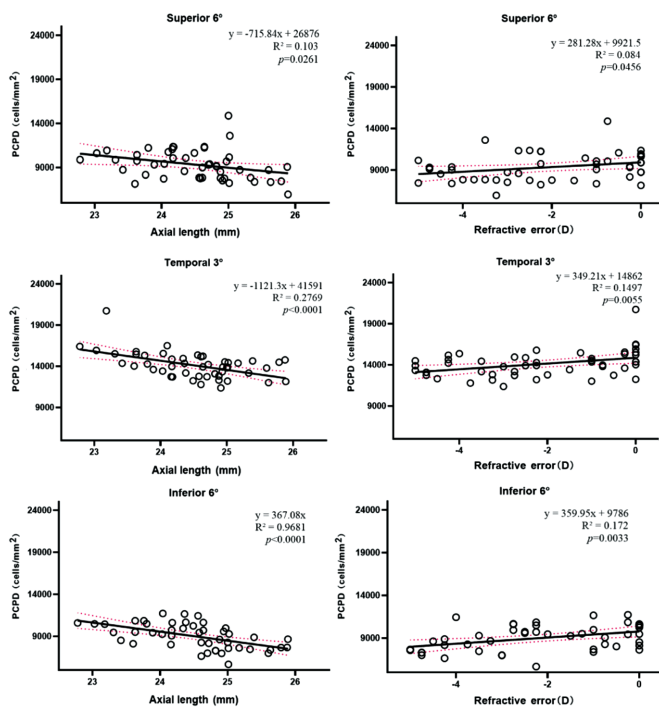


Figure 5 Variation of PCPD with different axial lengths and refractive errors All regression slopes were statistically significant ($P < 0.05$). PCPD: Photoreceptor cell packing density.

shown in Figures 5 and 6, respectively. The relationship between PCPD and cell spacing with AL and refractive error is depicted by solid lines in the linear regression analysis. The PCPD of the three eccentricities exhibited a significant correlation with diopter and ocular axis, and all regression slopes demonstrated statistical significance ($P < 0.05$). Additionally, a particularly robust correlation between cell density and AL was observed at the inferior 6°, yielding an

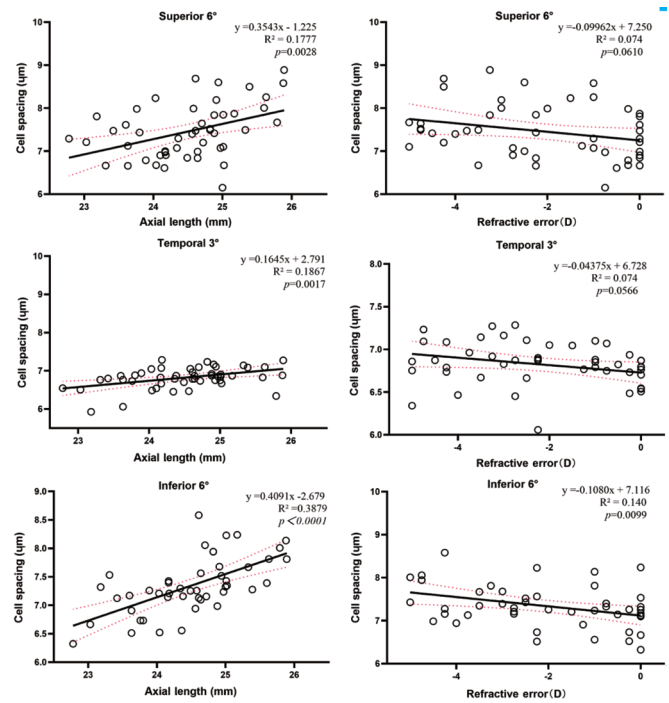


Figure 6 Variation of cell spacing with different axial lengths and refractive errors The correlation between all cell spacings and axial length was statistically significant. However, only the cell spacing at the inferior 6° exhibited statistical significance in its correlation with refractive error values ($P < 0.05$).

R^2 value of 0.9681. Unlike PCPD, as shown in Figure 6, cell spacing at the three locations was significantly correlated with AL ($P < 0.05$), while only at the inferior 6° was cell spacing significantly correlated with refractive error ($P < 0.05$). All regression slopes and equations were displayed within the figures.

DISCUSSION

In this study, we measured PCPD and cell spacing at temporal 3°, superior 6°, and inferior 6° in individuals with emmetropia, low myopia, and moderate myopia. The subjects were all healthy young Han Chinese adults aged between 20 and 30y. Our findings indicated a decreasing trend in PCPD and an increasing trend in cell spacing with increasing refractive error. Based on the observed correlation between PCPD, cell spacing, and AL, it can be inferred that these differences may be associated with ocular elongation, particularly at the inferior 6° position.

The modulation of photoreceptor function plays a crucial role in the progression of myopia^[20-21]. Additionally, the disruption in photoreceptor arrangement also suggests a dysregulation throughout the retinal visual pathway, thereby further exacerbating the progression of myopia. Our research findings suggested that moderate myopia (mean=-3.90, SD=0.82) exhibits a substantial reduction in PCPD along the temporal 3° and inferior 6° compared to emmetropic eyes (mean=-0.09, SD=0.16), whereas mild myopia (mean=-1.61, SD=0.68) exhibits a significant decrease solely in PCPD at 3° temporal to the fovea. Chui *et al*^[18] included 5 emmetropes and 6 individuals with myopia in their study, and also found a significant decrease in PCPD in eyes with increasing degree of myopia. This suggests a correlation between different degrees of myopia and varying distribution patterns of retinal photoreceptors. As the degree of myopia increases, there is an expansion in the range of alterations observed in PCPD. This trend indicates that, as the degree of myopia increases, the retinal photoreceptor cells undergo varying degrees of remodeling and adaptation.

Moreover, our investigation uncovers a correlation between AL and PCPD across the three retinal regions analyzed, surpassing that of refractive error. Assuming a stable complement of photoreceptors in adulthood, regions exhibiting differential PCPD attributable to AL disparities can be construed as sites of structural modification within ocular supportive tissues such as the Bruch's membrane and sclera^[22]. Stated differently, varying ALs correlate with disparities in the growth of the Bruch's membrane/sclera. This anatomical revelation substantiates the notion that these structures are pivotal in the ocular elongation characteristic of myopic progression^[22-25]. Furthermore, such elongation may precipitate choroidal thinning^[26] and alterations in retinal thickness^[27-28], thereby exerting an influence on the efficiency of visual transmission and the manifestation of visual function.

This study exclusively focuses on the changes in AL and PCPD after the onset of myopia. A reduction in PCPD was observed alongside changes in refractive status. However, the development of myopia is a multifaceted process involving

several factors, including ocular structure, function, and environmental influences. The challenges associated with the interpretation of PCPD changes in relation to myopia must be considered. Specifically, it remains unclear whether these alterations contribute to further myopia progression or are secondary changes linked to primary factors. The signals transmitted by cone cells disrupted by mutations regulate axial growth, and the LVAVA splicing defect mutation has been shown to be associated with both syndromic and non-syndromic myopia caused by excessive axial elongation^[29]. Photoreceptor cells play a critical role in refractive development during eye growth^[30], yet it is uncertain whether a decline in PCPD in adulthood might further influence eye growth and refractive status, thereby accelerating myopia progression. Additional longitudinal studies are necessary to establish whether PCPD changes actively drive myopia progression or simply serve as an indicator of the condition. A more comprehensive understanding of these mechanisms and their relative contributions could inform the development of more precise and effective myopia prevention and control strategies, addressing both primary and secondary factors to safeguard visual health.

Notably, our study revealed a stronger correlation between PCPD and AL at the inferior 6° location ($R^2=0.9681$) compared to the temporal 3° and superior 6° positions. This finding raises further questions about whether axial elongation in myopic eyes occurs uniformly or locally. We hypothesize that retinal elongation related to AL does not occur uniformly along the meridians, supporting the theory of localized retinal elongation. Jonas *et al*^[31] observed a decline in PCPD and total retinal thickness in patients with axial myopia, with the most pronounced decrease occurring in the posterior equatorial region, followed by the equator. Chui *et al*^[18] expanded retinal measurements by collecting cone density data along four major meridians, covering eccentricities from 0.30 to 3.40 mm (approximately 0.30° to 24°). Although their study had a small sample size, including only 11 human eyes, limiting the generalizability and statistical power of their conclusions, they similarly found evidence of localized retinal elongation. In contrast, Woog and Legras^[19] calculated the correlation between cone density and AL along the horizontal meridian in both myopic and emmetropic populations, finding that the retinal stretching along the horizontal meridian is uneven, further supporting the hypothesis of localized retinal elongation. While their study expanded the measurement range (3° to 24° eccentricities), it lacked sampling of the vertical meridian, a limitation addressed in the current study, which further validates the association between axial elongation and localized retinal stretching. Unfortunately, due to the limited vertical meridian sampling capability of our instruments, our

findings cannot definitively determine the role of vertical meridian elongation in overall axial elongation, and further research is needed to confirm these results.

Based on the strong correlation between PCPD and AL, the area 6° below the fovea may be a key target region for myopia intervention. Developing optical correction methods specifically designed for this area, such as specially designed lenses or contact lenses, could enable localized modulation of visual stimuli, potentially inhibiting abnormal axial elongation. Future research should increase the sample size to include subjects of varying ages, genders, and ethnic backgrounds to validate the generalizability of the current findings. Furthermore, the integration of advanced imaging techniques, such as OCT, can provide more precise measurements of retinal microstructural changes, offering deeper insights into the mechanisms underlying myopia progression^[32].

A limitation of this study is the absence of PCPD measurements at the fovea, which represents the pivotal region for spatial vision and poses challenges in imaging due to the diminutive size of photoreceptors, despite advancements in image quality. The quality of the images poses another limitation, particularly for eyes with a refractive error exceeding -5 D. Due to experimental precision constraints, discerning fine details remains challenging in the majority of cases. To ensure research accuracy, individuals with a spherical equivalent surpassing -5 D of myopia are excluded from our affiliated group.

In summary, the objective of our study is to develop a predictive model to assess the variation in PCPD among healthy young individuals with different refractive errors. Additionally, our findings demonstrate a declining trend in PCPD with increasing AL, accompanied by an increase in intercellular spacing. These foundational data hold significant implications as they may serve as effective tools for identifying and monitoring photoreceptor cell degeneration in retinal diseases.

ACKNOWLEDGEMENTS

Foundation: Supported by National Natural Science Foundation of China (No.82271107).

Conflicts of Interest: Lei LY, None; Zhao Y, None; Cai TR, None; Feng SG, None; Yao J, None.

REFERENCES

- 1 Baird PN, Saw SM, Lanca C, *et al.* Myopia. *Nat Rev Dis Primers* 2020;6:99.
- 2 Morgan IG, Ohno-Matsui K, Saw SM. Myopia. *Lancet* 2012;379(9827):1739-1748.
- 3 Holden BA, Fricke TR, Wilson DA, *et al.* Global prevalence of myopia and high myopia and temporal trends from 2000 through 2050. *Ophthalmology* 2016;123(5):1036-1042.
- 4 Du R, Xie SQ, Igarashi-Yokoi T, *et al.* Continued increase of

- axial length and its risk factors in adults with high myopia. *JAMA Ophthalmol* 2021;139(10):1096-1103.
- 5 Jonas JB, Bikbov MM, Wang YX, *et al.* Anatomic peculiarities associated with axial elongation of the myopic eye. *J Clin Med* 2023;12(4):1317.
- 6 Fricke TR, Holden BA, Wilson DA, *et al.* Global cost of correcting vision impairment from uncorrected refractive error. *Bull World Health Organ* 2012;90(10):728-738.
- 7 Heitkotter H, Salmon AE, Linderman RE, *et al.* Theoretical versus empirical measures of retinal magnification for scaling AOSLO images. *J Opt Soc Am A Opt Image Sci Vis* 2021;38(10):1400-1408.
- 8 Morgan JIW, Chui TYP, Grieve K. Twenty-five years of clinical applications using adaptive optics ophthalmoscopy. *Biomed Opt Express* 2023;14(1):387-428.
- 9 Pircher M, Zawadzki RJ, Evans JW, *et al.* Simultaneous imaging of human cone mosaic with adaptive optics enhanced scanning laser ophthalmoscopy and high-speed transversal scanning optical coherence tomography. *Opt Lett* 2008;33(1):22-24.
- 10 Wynne N, Carroll J, Duncan JL. Promises and pitfalls of evaluating photoreceptor-based retinal disease with adaptive optics scanning light ophthalmoscopy (AOSLO). *Prog Retin Eye Res* 2021;83:100920.
- 11 Roorda A, Romero-Borja F, Donnelly Iii W, *et al.* Adaptive optics scanning laser ophthalmoscopy. *Opt Express* 2002;10(9):405-412.
- 12 Curcio CA, Sloan KR, Kalina RE, *et al.* Human photoreceptor topography. *J Comp Neurol* 1990;292(4):497-523.
- 13 Brennan BD, Heitkotter H, Carroll J, *et al.* Quantifying image quality in AOSLO images of photoreceptors. *Biomed Opt Express* 2024;15(5):2849-2862.
- 14 Strang NC, Winn B, Bradley A. The role of neural and optical factors in limiting visual resolution in myopia. *Vision Res* 1998;38(11):1713-1721.
- 15 Jaworski A, Gentle A, Zele AJ, *et al.* Altered visual sensitivity in axial high myopia: a local postreceptor phenomenon? *Invest Ophthalmol Vis Sci* 2006;47(8):3695-3702.
- 16 Rossi EA, Weiser P, Tarrant J, *et al.* Visual performance in emmetropia and low myopia after correction of high-order aberrations. *J Vis* 2007;7(8):14.
- 17 Atchison DA, Schmid KL, Pritchard N. Neural and optical limits to visual performance in myopia. *Vision Res* 2006;46(21):3707-3722.
- 18 Chui TY, Song HX, Burns SA. Individual variations in human cone photoreceptor packing density: variations with refractive error. *Invest Ophthalmol Vis Sci* 2008;49(10):4679-4687.
- 19 Woog K, Legras R. Distribution of mid-peripheral cones in emmetropic and myopic subjects using adaptive optics flood illumination camera. *Ophthalmic Physiol Opt* 2019;39(2):94-103.
- 20 Hendriks M, Verhoeven VJM, Buitendijk GHS, *et al.* Development of refractive errors-what can we learn from inherited retinal dystrophies? *Am J Ophthalmol* 2017;182:81-89.
- 21 Huang YK, Chen X, Zhuang J, *et al.* The role of retinal dysfunction in myopia development. *Cell Mol Neurobiol* 2023;43(5):1905-1930.

- 22 Jonas JB, Jonas RA, Bikbov MM, *et al.* Myopia: histology, clinical features, and potential implications for the etiology of axial elongation. *Prog Retin Eye Res* 2023;96:101156.
- 23 Yan F, Hui YN, Li YJ, *et al.* Epidermal growth factor receptor in cultured human retinal pigment epithelial cells. *Ophthalmologica* 2007;221(4):244-250.
- 24 Vatsyayan R, Chaudhary P, Sharma A, *et al.* Role of 4-hydroxynonenal in epidermal growth factor receptor-mediated signaling in retinal pigment epithelial cells. *Exp Eye Res* 2011;92(2):147-154.
- 25 Liu HH, Gentle A, Jobling AI, *et al.* Inhibition of matrix metalloproteinase activity in the chick sclera and its effect on myopia development. *Invest Ophthalmol Vis Sci* 2010;51(6):2865-2871.
- 26 Yazdani N, Ehsaei A, Hoseini-Yazdi H, *et al.* Wide-field choroidal thickness and vascularity index in myopes and emmetropes. *Ophthalmic Physiol Opt* 2021;41(6):1308-1319.
- 27 Jonas JB, Dai Y, Panda-Jonas S. Peripapillary suprachoroidal cavitation, parapapillary gamma zone and optic disc rotation due to the biomechanics of the optic nerve dura mater. *Invest Ophthalmol Vis Sci* 2016;57(10):4373.
- 28 Chua SYL, Dhillon B, Aslam T, *et al.* Associations with photoreceptor thickness measures in the UK biobank. *Sci Rep* 2019;9(1):19440.
- 29 Neitz M, Neitz J. Intermixing the *OPN1LW* and *OPN1MW* genes disrupts the exonic splicing code causing an array of vision disorders. *Genes (Basel)* 2021;12(8):1180.
- 30 Wang KL, Han GG, Hao R. Advances in the study of the influence of photoreceptors on the development of myopia. *Exp Eye Res* 2024;245:109976.
- 31 Jonas JB, Spaide RF, Ostrin LA, *et al.* IMI-nonpathological human ocular tissue changes with axial myopia. *Invest Ophthalmol Vis Sci* 2023;64(6):5.
- 32 Jonas JB, Wang YX, Dong L, *et al.* Advances in myopia research anatomical findings in highly myopic eyes. *Eye Vis (Lond)* 2020;7:45.